Beam redirection and frequency filtering with transparent elastomeric diffractive elements

Bartosz A. Grzybowski, Dong Qin, and George M. Whitesides

A new, to our knowledge, type of optical device capable of beam redirection and frequency filtering is described. It is based on a transparent elastomeric binary diffraction grating. When light is passed through the device the intensities of the diffraction orders can be modulated by compression of the elastomer in the direction perpendicular to the plane of the grating. Selective filtering of the component frequencies of two-component light ($\lambda = 543.5$ nm and $\lambda = 632.8$ nm) has been demonstrated. Experimental observations are in agreement with theoretical calculations quantifying the performance of the device. © 1999 Optical Society of America

OCIS codes: 230.1950, 050.1940, 160.5470, 330.6180, 050.1970.

1. Introduction

This paper describes a new, to our knowledge, type of optical device that is capable of frequency filtering and beam redirection. The device is composed of a transparent elastomeric element with a binary grating that is a few micrometers deep and is embossed on its surface. When the elastomer is compressed in the direction perpendicular to the plane of the grating, the relative optical path of the light traveling through its raised and recessed regions changes. Thus compressing the elastomer modulates the intensities of diffraction orders. In addition, for a given compression the intensity of light diffracted into a particular order depends on the frequency of light. If nonmonochromatic light is used the ratios of the intensities of the component frequencies diffracted into a given order will vary with compression. To achieve efficient filtering, it is necessary for these ratios to be maximized: That is, at a given diffraction order the intensity of one of the component frequencies must predominate.

This paper shows that, with the elastomeric device we describe, highly selective filtering of two-component light ($\lambda = 543.5$, 632.8 nm in our study) is possible for values of compressive strains that are less than ~6%. Although other devices capable of optical filtering exist (tunable grid filters,[1] grating-based micromachined light modulators,[2–5] Fabry–Perot cavities,[6,7] prisms[8]), several characteristics of this new type of filter make it an attractive alternative to these more familiar systems: (i) It can be fabricated easily and inexpensively. (ii) The depth of the grating is easily controlled because the submicrometer changes in the depth of the grating required for operation require relatively large—of the order of tens of micrometers—deformations of the elastomer.

The paper is organized into three parts. First, we develop a simple theoretical description of the modulation of the intensity of light on passage through a compressible binary grating (some lengthy derivations are relegated to Appendix A). Second, we describe the fabrication of the device and the experimental methods used to measure its performance. Third, we summarize the experimental results and compare experiment to theory.

2. Theory

The grating is assumed to remain binary during compression. The transmission function $\tau(x)$ (see Fig. 1 for the coordinate system) is described by

$$\tau(x) = \begin{cases} \exp(i\phi) & \text{for } nL < x < \left(n + \frac{1}{2}\right)L, \\ 1 & \text{otherwise} \end{cases} \qquad (1)$$

$$n = 0, \pm 1, \pm 2, \ldots, \pm N/2$$

The authors are with the Department of Chemistry and Chemical Biology, Harvard University, 12 Oxford Street, Cambridge, Massachusetts 02138. G. M. Whitesides' e-mail address is gwhitesides@gmwgroup.harvard.edu.

Received 21 July 1998; revised manuscript received 23 November 1998.
0003-6935/99/142997-06$15.00/0
© 1999 Optical Society of America

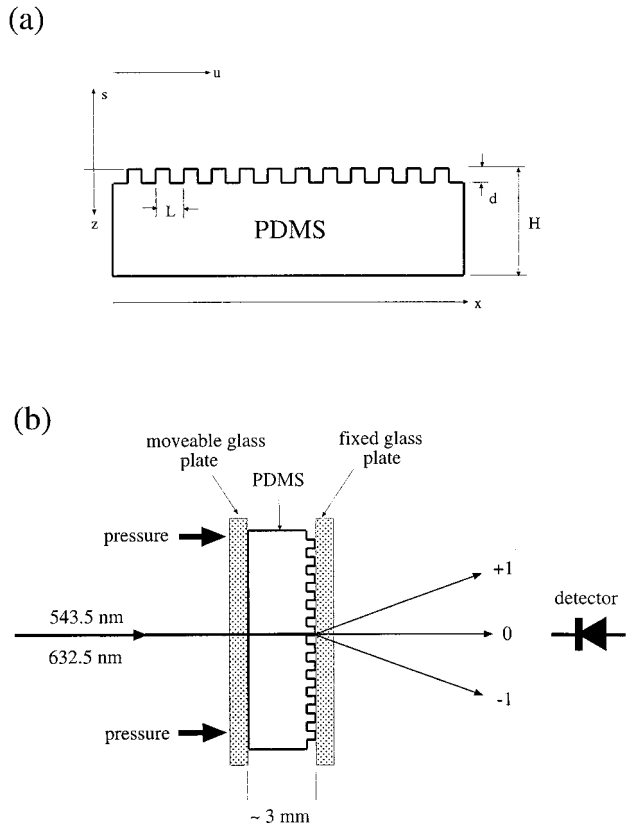

Fig. 1. (a) Coordinates used in the calculations. (b) Scheme of the experimental setup. PDMS, polydimethylsiloxane.

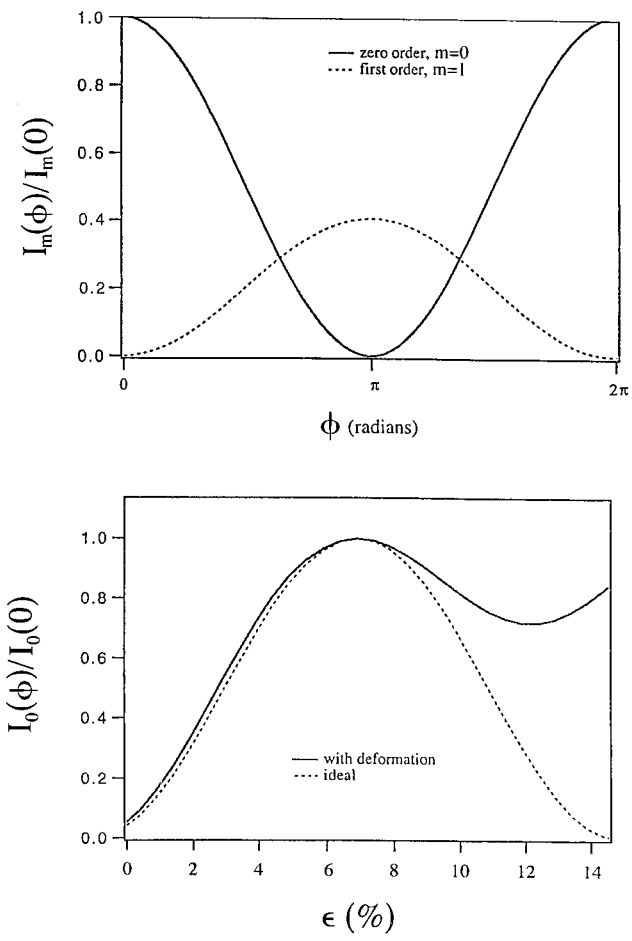

Fig. 2. (a) Calculated dependence of the intensities of the zero and the first orders as functions of the phase angle. (b) Effect of the deformation of the grating during compression on the intensity of the zero-order beam. Even with a conservative estimate of the constant, $C = 20$, the intensity curves with and without the stress correction are in good agreement across the operational range of the device ($\epsilon < \sim 6\%$). In both cases the calculations were carried out with values of $d_0 = 1.8$ μm and $\lambda = 543.5$ nm.

where ϕ is the depth of modulation of the phase in radians and L is the period of the grating. We assume that the optical field is a plane wave before it passes through the grating and that the number of the grating lines $N + 1$ is large. The Fraunhofer complex-amplitude distribution $U(f)$ is given by the Fourier transform of the transmission function evaluated at the spatial frequency of $f = u/s\lambda$, where λ is the wavelength of light, s is the distance between the plane of the grating and the plane at which the diffraction is calculated, and u is the coordinate along this plane[9,10]:

$$U(f) = \int_{-(N+1)L/2}^{(N+1)L/2} \tau(x)\exp(-i2\pi xf)\mathrm{d}x = \sum_{m=-N/2}^{m=N/2} \int_{mL-L/2}^{mL+L/2} \tau(x)\exp(-i2\pi xf)\mathrm{d}x. \quad (2)$$

Substituting $y = x - mL$ into Eq. (2) and in the limit of $N \to \infty$, we obtain Eq. (3) (see Appendix A for derivation) in which δ is the delta function:

$$U(f) = \sum_{m=-\infty}^{\infty} \delta\left(f - \frac{m}{L}\right) \frac{1}{L} \int_{-L/2}^{L/2} \tau(y)\exp(-i2\pi yf)\mathrm{d}y. \quad (3)$$

The diffraction orders are located at $u = m\lambda s/L$ [Eq. (3)], and the intensity of the mth order is equal to the square of the modulus of the Fraunhofer complex-amplitude distribution, as given by Eq. (4), below [$U_m(f)$ stands for $U(f)$ when evaluated for a particular value of m]. The intensities of the zeroth [$m = 0$, $I_0(f)$] and the first [$m = \pm 1$, $I_1(f)$] diffraction orders are given by

$$I_m(f) = |U_m(f)|^2 = \frac{1}{L^2}\left|\int_{-L/2}^{L/2} \tau(y)\exp(-i2\pi ym/L)\mathrm{d}y\right|^2 \quad (4)$$

and are calculated by use of Eqs. (1) and (4) (see Appendix A) to demonstrate that changing the depth of modulation of the phase ϕ changes the intensities

of the diffraction orders [note that the intensity is now written as a function of the phase; Fig. 2(a)]:

$$I_0(\phi) = \frac{1 + \cos\phi}{2}, \tag{5a}$$

$$I_1(\phi) = \frac{2(1 - \cos\phi)}{\pi^2}. \tag{5b}$$

The magnitude of the phase ϕ depends on the depth of the grating d, the wavelength of the diffracted light λ, and the indices of refraction of the elastomer n_e [1.43 for polydimethylsiloxane (PDMS)] and of air n_{air}:

$$\phi = \frac{2\pi(n_e - n_{\text{air}})d}{\lambda}. \tag{6}$$

Because d changes on compression, the phase ϕ is a function of the degree of compression: $\phi(d) = \phi(d_0) + \Delta\phi$ (d_0 is the depth of the uncompressed grating). Using Eq. (6), we can write $\Delta\phi$ as

$$\Delta\phi = \frac{2\pi(n_e - n_{\text{air}})(d - d_0)}{\lambda} = \frac{2\pi\Delta n\Delta d}{\lambda}. \tag{7}$$

For small compressions, we assume the change in the depth of the surface relief Δd to be proportional to the z displacement (in the direction perpendicular to the plane of the grating) of an element with a flat surface at a depth equal to the depth of the uncompressed relief: $\Delta d \propto \mathrm{d}z$ ($z = d_0$). Using this proportionality and the relations for stress and strain (see Appendix A), we obtain the dependence of the change in optical phase on the compressive strain $\epsilon = \Delta H/H$ [see Eq. (8), below], where ΔH is the change in the thickness of the elastomer on compression,

$$\Delta\phi \propto \frac{2\pi\Delta n d_0}{\lambda}\frac{\Delta H}{H}, \tag{8}$$

and H is the thickness of the elastomer in the uncompressed state.

Equations (5a) and (5b) and expression (8) provide us with a description of the ideal optical response of the system during compression. Although these expressions do not take into account other deformations of the grating (e.g., widening, buckling, or wiggling of the grating lines), they accurately describe the performance of the device for compressive strains less than, for example, 6% (and for aspect ratios of the grating lines that are less than, for example, 1.1, when wiggling is not expected to be a major issue). It was shown previously by finite-element calculations[11,12] that, for as much as ~10% compressive strain, the grating retains a square wave shape. Therefore we considered a simple qualitative model in which the grating lines, as they are being compressed along the z (vertical) direction, expand in the x (horizontal) direction and retain a rectangular cross section. If we assume that, for small compressive strains, the horizontal expansion of the grating lines Δx is proportional to the vertical compression $d - d_0$ and, consequently, to the compressive strain ϵ, Eqs. (9a) and (9b) for the corrected intensities of the zero and the first orders, respectively, are derived (see Appendix A for details) as

$$I_{0,\text{corr}}(\phi) = \frac{1 + \cos\phi}{2} + C\epsilon^2(1 - \cos\phi), \tag{9a}$$

$$I_{1,\text{corr}}(\phi) = \frac{2}{\pi^2}\cos^2(\pi\epsilon\sqrt{C/2})(1 - \cos\phi). \tag{9b}$$

The value of the constant C can be estimated from the experimental zero-order intensity curves by the subtraction of the ideal contribution, $I_0(\phi) = (1 + \cos\phi)/2$, and the fitting of C to the resultant curve; in our experiments $C \sim 10$. For this value of C, the maximum difference between $I_{0,\text{corr}}(\phi)$ and $I_0(\phi)$ does not exceed 0.07 {in the worst-case situation, when $\cos[\phi(\epsilon = 0.06)] = -1$}, and between $I_1(\phi)$ and $I_{1,\text{corr}}(\phi)$ it is, at most, 0.068. Although for higher strains these differences become much larger [Fig. 2(b)], the ideal equations (5a) and (5b) describe the optical response of the device well over its operational range ($\epsilon < \sim 6\%$).

3. Fabrication and Experimental Protocol

We fabricated the elastomeric gratings (2-μm lines that are separated by 2 μm) by casting and curing a prepolymer of PDMS against photolithographically patterned lines of photoresist on silicon wafers.[13–15] The thickness of the patterns was controlled by adjustment of the spinning rate at which the photoresist (Shipley, photoresist 1822, maximum thickness of ~3 μm) was applied: for thicknesses of 1.8, 2.2, and 2.6 μm, the spin rates were 5500, 4000, and 3000 rpm, respectively, for 40 s. The UV exposure times for such photoresist-coated silicon wafers were 5.5, 6.5, and 7.5 s, respectively. After the PDMS was cast against the patterns and cured, it was gently peeled away. In this way, we obtained transparent samples of the elastomer ($H \approx 3$ mm) with binary gratings (1.8, 2.2, and 2.6 μm deep) embossed on the surface.

The elastomer was placed between two glass plates: one fixed and the other attached to a translational stage moving in the direction perpendicular to the plane of the grating. For minimizing shear on the grating during compression the plates were parallel aligned by the temporary placement of silver-coated mirrors ($T \sim 30\%$) on the glass plates. The resulting assembly constituted a Fabry–Perot cavity that could be adjusted so that the multiple reflection spots overlapped. Two collinear laser beams (green at 543.5 nm and red at 632.8 nm) were passed through the sample. The intensities of the diffraction spots were monitored with silicon photodiode detectors [Fig. 1(b)].

4. Results and Discussion

The results are summarized in Figs. 3 and 4. The measured intensities of the zero-order spots were normalized to unity [maximum of the function $I_0(\phi)$,

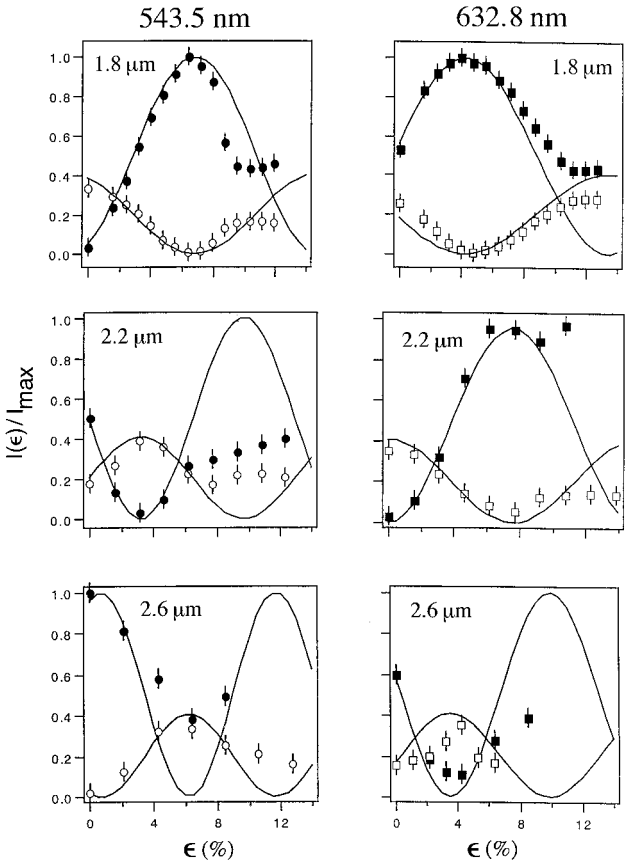

Fig. 3. Intensities of the zero and the first orders as functions of the compressive strain ϵ. The filled circles represent the zero order, and the open circles the first order results. The curves show the theoretical values.

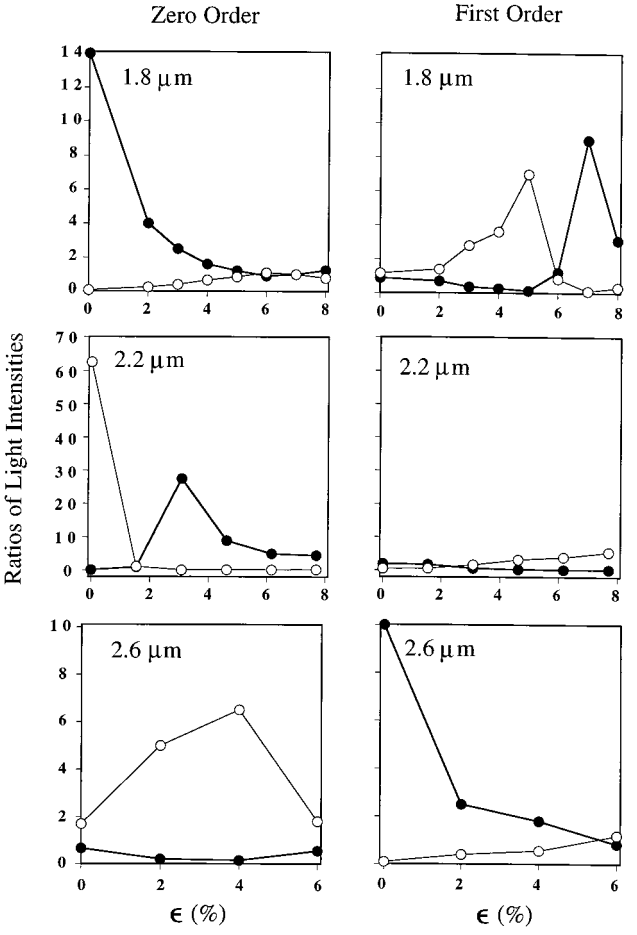

Fig. 4. Ratios of the intensities of the red to the green beams (filled circles) and the green to the red beams (open circles) when diffracted into the zero and the first orders.

cf. Eq. (5a)], and the first-order intensities were then plotted on the same scale. For 1.8- and 2.2-μm-deep gratings the experimental curves of the intensity versus the compressive strain agree with the theoretical ones for strains of as much as approximately 6%. The agreement is poor for the 2.6-μm grating. This result was expected because the high aspect ratio of the grating lines (1.3:1) will lead to buckling and shear distortions of the lines that will cause the assumption of a binary grating to break down (our simple theory does not attempt to describe these distortions). The modulation of the intensity of light was efficient (~17 dB) for 1.8- and 2.2-μm gratings. For these two gratings monochromatic light (red or green) can be directed selectively into either the zero or the first diffraction order, depending on compressive strain.

The relative wavelength-selectivity characteristics of the device are presented in Fig. 4. For the 1.8-μm grating and low compressive strains mostly red light is filtered into the zero order. With increasing strain the intensity of green light increases, reducing the efficiency of filtering. In the first order, at a compressive strain of approximately 5%, the intensity of green light becomes greater than that of red light, and at a compressive strain of approximately 7% the opposite is true. For the 2.2-μm grating the selectivity of diffraction into the zero order is better. At 0% strain the intensity of green light is more than 60 times greater than that of red light (18 dB). For a compressive strain of approximately 3% the opposite is true: red light is now approximately 30 times more intense than green (14.8 dB). Poor filtering into the first order (7 dB) is observed at higher strains (e.g., approximately 8%). Filtering is not efficient for a grating that is 2.6 μm thick (a maximum of 10 dB at 0% strain in the first order) or thicker.

The device can be used to filter wavelengths other than those used in our study. Figure 5 shows plots of the theoretical intensities of light filtered into the zero order as a function of both the wavelength (in the visible) and the compressive strain. The 1.8-μm grating [Fig. 5(a)] is selective not only for red–green, but also for blue–green dicomponent light. The 2.2-μm grating, on the other hand, can differentiate best between blue and red light. The selectivity for these three hues could be useful in constructing red–green–blue displays. In fact, one could envision a display built from small elastomeric pixels that differ in the depths of the gratings embossed on their surfaces. On selective compression of the pixels the

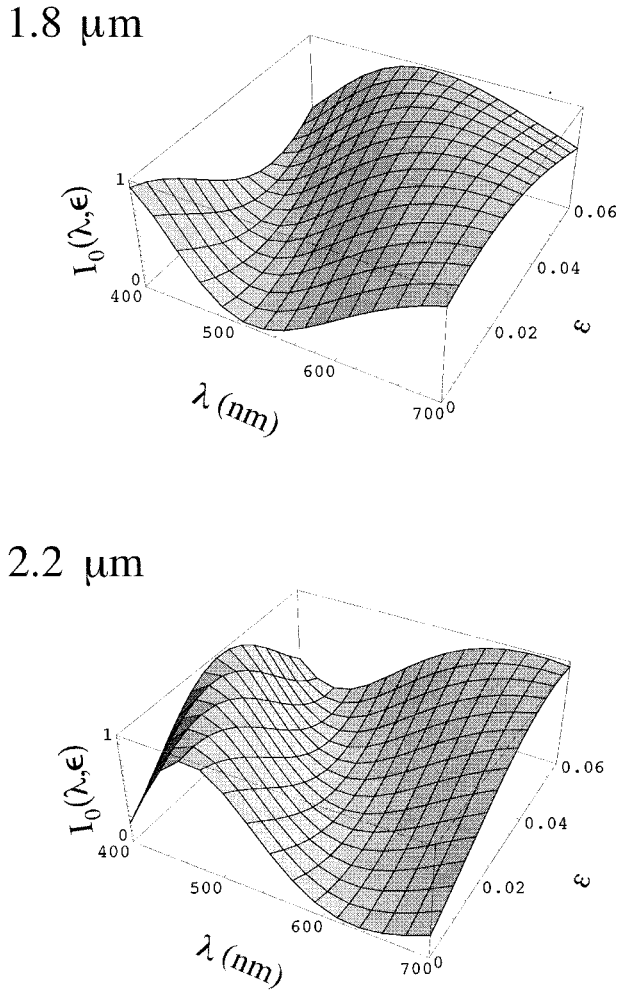

Fig. 5. Plots of the theoretical intensities of light filtered into the zero order as a function of both the wavelength (in the visible) and the compressive strain ϵ for the 1.8-μm grating and the 2.2-μm grating. The calculations were carried out by use of Eq. (9a) with a value for the constant of $C = 10$.

transmitted image could be modulated. In addition, topographies other than binary gratings might be used to give more elaborate diffraction patterns. For continuous tunable light sources the wavelength selectivity is poor: On the basis of the calculations, the bandwidth for low stresses would be ~100 nm, a value that prohibits the use of our device as a conventional bandpass filter.

The device described in this paper is easy to fabricate, inexpensive, and durable. It can serve as a pressure sensor, as a beam director, or as an optical filter. One can tune its characteristics by changing the dimensions (or the properties) of the elastomeric diffractive element. The performance of the device is optimal when the stress is uniaxial in the direction perpendicular to the plane of the grating. When the aspect ratio of the grating is high, shear stresses are hard to control, and the spectral purity of the filtered light decreases.

Appendix A

A. Derivation of Equation (3)

On substitution of $y = x - mL$ into Eq. (3), we obtain

$$U(f) = \sum_{m=-N/2}^{m=N/2} \exp(-i2\pi fmL) \times \int_{-L/2}^{L/2} \tau(y)\exp(-i2\pi fy)\mathrm{d}y.$$

In the limit of very large N, we have

$$U(f) = \lim_{N\to\infty} \sum_{m=-N/2}^{m=N/2} \exp(-i2\pi fmL) \times \int_{-L/2}^{L/2} \tau(y)\exp(-i2\pi fy)\mathrm{d}y,$$

and, by evaluating the sum, we obtain

$$U(f) = \lim_{N\to\infty} \frac{\sin[\pi fL(N+1)]}{\sin(\pi fL)} \int_{-L/2}^{L/2} \tau(y)\exp(-i2\pi fy)\mathrm{d}y.$$

If we note that

$$\lim_{N\to\infty} \frac{\sin[\pi fL(N+1)]}{\sin(\pi fL)} = \sum_{m=-\infty}^{m=\infty} \frac{1}{L}\,\delta\left(f - \frac{m}{L}\right),$$

Eq. (3) is obtained.

B. Derivation of Equations (5)

We derive Eqs. (5) as follows:

$$\begin{aligned} I_0(\phi) &= \frac{1}{L^2}\left[\int_{-L/2}^{L/2} \tau(y)\mathrm{d}y\right]\left[\int_{-L/2}^{L/2} \tau^*(y)\mathrm{d}y\right] \\ &= \frac{1}{L^2}\left[\frac{L}{2} + \frac{L}{2}\exp(i\phi)\right]\left[\frac{L}{2} + \frac{L}{2}\exp(-i\phi)\right] \\ &= \frac{1}{4}[2 + \exp(i\phi) + \exp(-i\phi)] \\ &= \frac{1 + \cos\phi}{2}, \end{aligned}$$

$$\begin{aligned} I_1(\phi) &= \frac{1}{L^2}\left[\int_{-L/2}^{L/2} \tau(y)\exp\left(\frac{-i2\pi y}{L}\right)\mathrm{d}y\right] \times \left[\int_{-L/2}^{L/2} \tau^*(y)\exp\left(\frac{i2\pi y}{L}\right)\mathrm{d}y\right] \\ &= \frac{1}{L^2}\frac{L^2}{\pi^2}[1 - \exp(i\phi)][1 - \exp(-i\phi)] \\ &= \frac{1}{\pi^2}\{2 - [\exp(i\phi) + \exp(-i\phi)]\} \\ &= \frac{2(1 - \cos\phi)}{\pi^2}. \end{aligned}$$

C. Derivation of Proportion (8)

For linear elastic materials a uniform axial stress in the z direction T_ϵ produces a uniform axial strain ϵ_z given by $T_\epsilon = E\epsilon_z$, where E is the Young's modulus. The z displacements throughout the elastomer are given by

$$\mathrm{d}z = -\frac{T_z}{E} z,$$

where $z = 0$ corresponds to the fixed glass plate. Because

$$\Delta\phi = \frac{2\pi\Delta n\Delta d}{\lambda}, \qquad \Delta d \propto \mathrm{d}z, \qquad z = d_0,$$

it follows that

$$\Delta\phi \propto \frac{2\pi\Delta n}{\lambda} d_0\epsilon_z.$$

Because $\epsilon_z = \Delta H/H$, we can also write

$$\Delta\phi \propto \frac{2\pi\Delta n d_0\Delta H}{\lambda H}.$$

We found the proportionality constant, which had a value of 4.963, by fitting to one of the experimental curves (the reference curve in our experiments for the 1.8-μm grating for zero-order green light).

D. Derivation of Equations (9a) and (9b)

Let Δx be the expansion of a grating line during compression. We assume that Δx is proportional to the compressive strain, i.e., $\Delta x = c_1\epsilon$. The transmission function for the compressed grating can be written as

$$\tau(x) = \begin{cases} \exp(i\phi) & \text{for } nL - \dfrac{\Delta x}{2} < x < \left(n + \dfrac{1}{2}\right)L + \dfrac{\Delta x}{2} \\ & n = 0, \pm 1, \pm 2, \ldots, \pm N/2 \\ 1 & \text{otherwise} \end{cases}.$$

The intensity of the zero order calculated from Eq. (4) by use of this transmission function (with $y = x$) is

$$I_{0,\mathrm{corr}}(\phi) = \frac{1}{L^2}\left|\int_{-L/2}^{L/2} \tau(y)\mathrm{d}y\right|^2$$
$$= \frac{1}{L^2}\left|\left(\frac{L}{2} - \Delta x\right) + \left(\frac{L}{2} + \Delta x\right)\exp(i\phi)\right|^2,$$

which, after some algebra, leads to Eq. (9a):

$$I_{0,\mathrm{corr}}(\phi) = \frac{1 + \cos\phi}{2} + C\epsilon^2(1 - \cos\phi),$$

where $C = 2c_1{}^2/L^2$ is a constant. The intensity of the first order [Eq. (9b)] is obtained by a similar procedure (with $y = x - L$):

$$I_{1,\mathrm{corr}}(\phi) = \frac{1}{L^2}\left|\int_{-L/2}^{L/2} \tau(y)\exp\left(\frac{-\pi 2iy}{L}\right)\mathrm{d}y\right|^2$$
$$= \frac{1}{L^2}\left|\frac{iL}{\pi}\cos\left(\frac{\pi\Delta x}{L}\right)[1 - \exp(i\phi)]\right|^2$$
$$= \frac{2}{\pi^2}\cos^2[\pi\epsilon(C/2)^{1/2}](1 - \cos\phi).$$

This study was supported by the Defense Advanced Research Project Agency and by the National Science Foundation under award ECS-9729405.

References

1. T. R. Ohnstein, J. D. Zook, H. B. French, H. Guckel, T. Earles, J. Klein, and P. Magnat, "Tunable IR filters with integral electromagnetic actuators," in *Proceedings of the Solid State Sensor and Actuator Workshop* (Elsevier, Lausanne, Switzerland, 1996), pp. 196–199.
2. O. Solgaard, F. S. A. Sandejas, and D. M. Bloom, "Deformable grating optical modulator," Opt. Lett. **17,** 688–690 (1992).
3. C. Cremer, N. Emeis, M. Schier, G. Heise, G. Ebbinghaus, and L. Stoll, "Grating spectrograph integrated with photodiode array in InGaAsP/InGaAs/InP," IEEE Photon. Technol. Lett. **4,** 108–110 (1992).
4. G. M. Yee, P. A. Hing, N. I. Maluf, and G. T. A. Kovacs, "Miniaturized spectrometers for biochemical analysis," in *Proceedings of the Solid State Sensor and Actuator Workshop* (Elsevier, Lausanne, Switzerland, 1996), pp. 64–67.
5. T. A. Kwa and R. F. Wolffenbuttel, "Integrated grating/detector array fabricated in silicon using micromachining techniques," Sensors Actuators A **31,** 259–266 (1992).
6. J. H. Jerman, D. J. Clift, and S. R. Mallison, "A miniature Fabry–Perot interferometer with a corrugated silicon diaphragm support," Sensors Actuators A **29,** 151–158 (1991).
7. K. Aranti, P. J. French, P. M. Sarro, D. Poenar, R. F. Wolffenbuttel, and S. Middelhoek, "Surface micromachined tunable interferometer array," Sensors Actuators A **43,** 17–23 (1994).
8. R. L. Fork, "Optical frequency filter for ultrashort pulses," Opt. Lett. **11,** 629–631 (1986).
9. M. Born and E. Wolf, eds., *Principles of Optics*, 6th ed. (Pergamon, Oxford, 1980), Chaps. 8.6.1, 8.6.3.
10. K. Iizuka, *Engineering Optics*, 2nd ed. (Springer-Verlag, Berlin, 1987), pp. 59–65.
11. J. A. Rogers, D. Qin, O. J. A. Schueller, and G. M. Whitesides, "Elastomeric binary phase gratings for measuring acceleration, displacement, strain and stress," Rev. Sci. Instrum. **67,** 3310–3319 (1996).
12. J. A. Rogers, O. J. A. Schueller, C. Marzolin, and G. M. Whitesides, "Wave-front engineering by use of transparent elastomeric optical elements," Appl. Opt. **36,** 5792–5795 (1997).
13. Y. Xia and G. M. Whitesides, "Soft lithography," Angew. Chem. Inter. Ed. Engl. **37,** 550–575 (1998).
14. A. Kumar and G. M. Whitesides, "Features of gold having micrometer to centimeter dimensions can be formed through a combination of stamping with an elastomeric stamp and an alkanethiol ink followed by chemical etching," Appl. Phys. Lett. **63,** 2002–2004 (1993).
15. A. Kumar, H. A. Biebuyck, and G. M. Whitesides, "Patterning self-assembled monolayers: applications in material science," Langmuir **10,** 1498–1511 (1994).